

Tunnel crisis and the crisis-induced intermittency

H. L. Yang

*China Center of Advanced Science and Technology (World Laboratory), P.O. Box 8730, Beijing 100080, China
and Institute of Low Energy Nuclear Physics, Beijing Normal University, Beijing 100875, China*

Z. Q. Huang

Institute of Low Energy Nuclear Physics, Beijing Normal University, Beijing 100875, China

E. J. Ding

*China Center of Advanced Science and Technology (World Laboratory), P.O. Box 8730, Beijing 100080, China;
Institute of Low Energy Nuclear Physics, Beijing Normal University, Beijing 100875, China;
and Institute of Theoretical Physics, Academia Sinica, Beijing, 100080, China*

(Received 15 October 1996)

In this paper a different type of crisis in random map is studied. The trigger of this crisis is the tunnel effect induced by a backward tangent bifurcation, while the previously reported crises are all caused by the collision of the chaotic attractor with an unstable orbit. In studying the intermittency behaviors induced by the crisis, two different characteristic times are defined. The scaling laws of the characteristic times are calculated numerically. Comparing the present crisis with the previously reported cases, the difference between their mechanisms is shown. Corresponding to this difference, two groups of crises are classified.

[S1063-651X(97)01106-9]

PACS number(s): 05.45.+b

I. INTRODUCTION

A central problem in nonlinear dynamics is that of discovering how the qualitative dynamical properties of orbits change and evolve as a dynamical system is continuously changed. The period-doubling bifurcation cascade, intermittency, crisis, and basin boundary metamorphoses are some examples of this type of transition in the dynamical behavior with the variation of a parameter [1]. One of them, crisis, has played a prominent role in the understanding of chaos. It names the discontinuous change of the chaotic attractor in phase space and is caused by the collision of the chaotic attractor with an unstable attractor or, equivalently, its stable manifold. During the past couple of decades, much work has been done on this subject [2–8]. Corresponding to the discontinuous change in the chaotic attractor induced by crises, Grebogi and co-workers named the crisis the boundary crisis, interior crisis, and merging crisis, respectively [3]. For a properly defined characteristic time τ , the mean characteristic time exhibits perfect power-law relation as $\langle \tau \rangle \sim \epsilon^\gamma$ with the variation of the control parameter ϵ . A theoretical approach to obtain the critical exponent γ of the crisis in two-dimensional dissipative systems was developed by Grebogi *et al.* [3]. Also, rich behaviors in high-dimensional systems have been studied by different authors [6–8].

Recently, a different mechanism of crisis in a random map has been reported [9]. In this case the crisis is triggered by a backward tangent bifurcation that is induced by the random variation of a parameter. Due to the tangent bifurcation, a narrow tunnel appears randomly between the graph of the map and the 45° line. Then the phase points are able to escape via this tunnel from the original region where they stayed. This mechanism is different from that of the formerly reported cases of crises that are caused by the collision of the chaotic attractor with an unstable orbit.

In this paper, some simple models that can exhibit this crisis are given. Also the intermittency behaviors induced by the new crisis are studied. This paper is organized as follows: In Sec. II, some simple models that can exhibit the present crisis are given. In Sec. III, two characteristic times τ_1 and τ_2 are defined. The scaling laws of the characteristic times with respect to the variation of the parameter are also studied here. Section IV is a short summary and discussion. We show the difference between the present crisis and the previously reported crises. Corresponding to the difference in their mechanisms, two groups, named “tunnel crisis” and “collision crisis,” are classified. The reasons why the characteristic times of the intermittency behavior are very long are given.

II. MODELS

In this section, three simple examples that can exhibit the present crisis will be studied. Two of them are randomly driven maps. The third one is a chaotically driven ordinary differential equation (ODE). One of our motivations to study such a randomly (or chaotically) driven system is to understand the mechanism of the synchronization of chaotic systems [10]. For the chaotic synchronization, there is always an ensemble of identical nonlinear systems driven by a chaotic signal. So the study of a single random driven system is important to the understanding of the mechanism of chaotic synchronization. This work is also motivated by the attempt to study the domain loss of a multiperiodic system under the influence of random driving [11–14]. Some authors even have noted that the domain loss under the influence of noise results from a crisislike behavior.

The first model we study is just a randomly shifted map with the form

$$y_{n+1} = f(f(y_n)) + z_n \pmod{1}, \quad (2.1)$$

where

$$f(y) = ay(1 - y), \tag{2.2}$$

$$z_n = bx_n, \tag{2.3}$$

and x_n ($n = 1, 2, 3, \dots$) are a series of random numbers homogeneously distributed in the interval $[0, 1]$, and a, b are two positive real constants.

For $a = 3.2, b = 0$, the system has two coexisting fixed points $y_{0,1}^s = 0.513$ and $y_{0,2}^s = 0.8$. Here $y_{b,i}$ is the i th root of the equation $f(f(y)) + b = y$ when all its nonzero roots are arranged in ascending order. Other symbols of y with subscripts of similar meaning are used in this paper. The stability of the state is indexed by the superscripts s and u , respectively. For identical systems starting from different initial points, they finally evolve to one of the two states. The basin boundary of the two states is the unstable fixed point $y_0^u = 0.688$ of $f(f(y)) = y$.

If we fix the value of a and increase the noise strength b slowly, the graph of the map at different steps is blurred into a band bounded by

$$y_{n+1} = f(f(y_n)) \tag{2.4}$$

and

$$y_{n+1} = f(f(y_n)) + b \pmod{1}. \tag{2.5}$$

The two fixed points $y_{b,1}^s, y_{b,2}^s$ are blurred into two bands correspondingly. For simplicity, below we will denote the two bands evolved from $y_{b,1}^s$ and $y_{b,2}^s$ as the lower and the upper band, respectively. At this time, an ensemble of identical systems starting from different initial points still evolves to two distinct groups, although the orbit of a single system is already of weak random character. But it should be noted that an uncertain region appears between the basins of the two states. The boundary points y_b^u and y_0^u of the uncertain region are the unstable fixed points of $y_{n+1} = f(f(y_n)) + b \pmod{1}$ and $y_{n+1} = f(f(y_n))$. For an orbit starting from the phase point in this region, it is much more difficult to determine which state it finally evolves to. In Sec. IV it will be discussed in detail that the uncertain region plays an essential role in the present crisis. With the further increase of b , the fixed point $y_{b,1}^s$ and the unstable fixed point y_b^u approach each other. They eventually annihilate due to a backward tangential bifurcation as b reaches a critical value b_c (see Fig. 1). After that a narrow tunnel occasionally appears between the graph of the map and the 45° line. Then the orbits that are originally bounded in the lower band are able to escape to a larger region via this tunnel. The two bands change their sizes suddenly and merge into a single band. This sudden change of band size is another type of crisis named tunnel crisis [9]. The two typical orbits for the subcritical and the supercritical case are shown in Fig. 2.

The second model is a randomly shifted piecewise linear map

$$y_{n+1} = f(y_n) + z_n \pmod{1}, \tag{2.6}$$

where

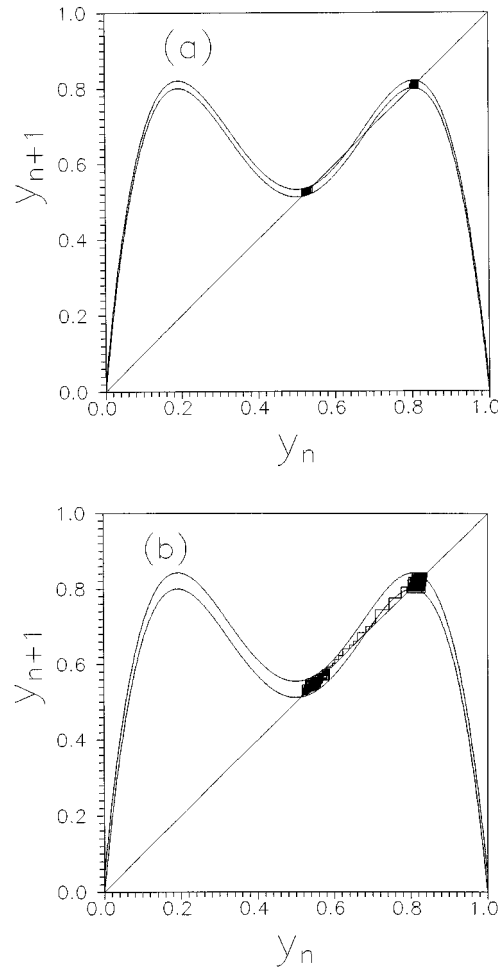


FIG. 1. (a) Orbits for the randomly shifted map (2.1) with $b = 0.02 < b_c$. The two orbits are bounded respectively in two separated bands. (b) Orbit for the map (2.1) with $b = 0.043 > b_c$ starting from the lower band. The orbit bounced back and forth randomly and transmitted finally to the higher band through the tunnel appearing between the graph of the map and the 45° line.

$$f(y) = \begin{cases} 5y/3 & \text{if } 0 \leq y < 1/5 \\ 1/3 & \text{if } 1/5 \leq y < 2/5 \\ 5y/3 - 1/3 & \text{if } 2/5 \leq y < 3/5 \\ 2/3 & \text{if } 3/5 \leq y < 4/5 \\ 5y/3 - 2/3 & \text{if } 4/5 \leq y < 1, \end{cases} \tag{2.7}$$

$$z_n = bx_n, \tag{2.8}$$

x_n is a series of random numbers homogeneously distributed in the interval $[0, 1]$, and b is a positive real constant. The motivation to study such a system is to compare it with the first model. The two models belong to two different metric universality classes. We want to know whether the critical exponent for the scaling law of the characteristic time is influenced by the form of the map.

The system has two fixed points $y_1^s = 1/3$ and $y_2^s = 2/3$ without the influence of the noise. The two fixed points are blurred into two bands with the slow increase of the noise strength b . The lower band loses its stability when b is beyond a critical value $b_c = x^* - y^*$. Here $y^* = 1/3$ and

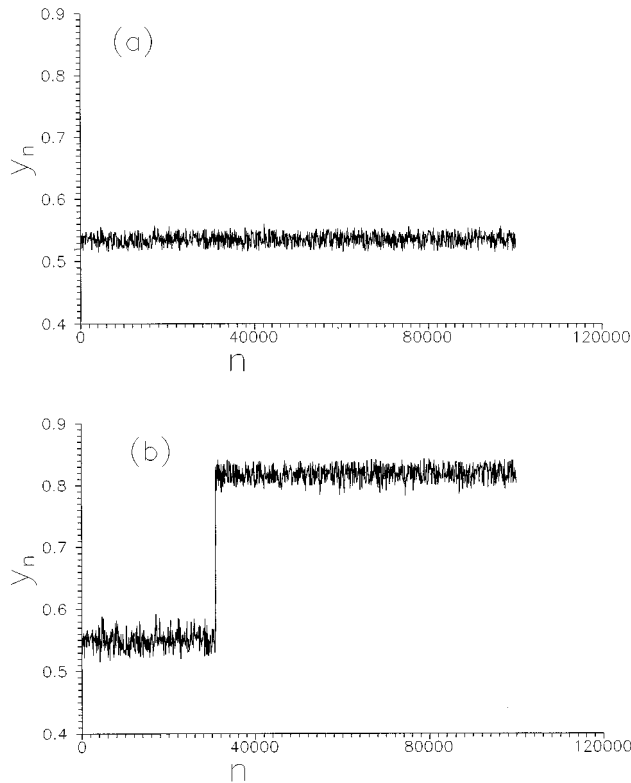


FIG. 2. y_n versus n of model (2.1) for the different values of b : (a) $b=0.02$; (b) $b=0.043$.

$x^*=2/5$ are just the coordinates of the tangent point (see Fig. 3). Via the randomly appeared narrow tunnel between the graph of the map and the 45° line, orbits originally bounded in the lower band finally escape. Figures 4(a) and 4(b) show the two typical orbits for b of the values below and above the critical value b_c , respectively.

The third model is a system of ODEs

$$\frac{dx_1}{dt} = 3x_1 - x_1^3 + b\sin(x_2/2), \quad (2.9)$$

$$\frac{dx_2}{dt} = x_3, \quad (2.10)$$

$$\frac{dx_3}{dt} = -0.22x_3 - \sin x_2 + 2.7\sin t. \quad (2.11)$$

If one divides the system into two subsystem x_1 and (x_2, x_3) , the subsystem (x_2, x_3) evolves chaotically for the given parameters. Since the subsystem (x_2, x_3) has no dependence on the variable x_1 , the whole system can be viewed as a chaotically driven one-dimensional ODE. The subsystem (x_2, x_3) is just the signal source to product a chaotic noise. For $b=0$, i.e., without the influence of the chaotic noise, the subsystem x_1 is bistable. It has two stable states $x_1^s = \pm\sqrt{3}$. With the increase of the noise magnitude b , the two fixed points are blurred into two bands distributed symmetrically at the two sides of the point $x_1=0$. The two bands change their size suddenly and merge into a single band as b passes through a critical value $b_c=2.0$. As a result, the orbit that is originally bounded in the region of positive (or

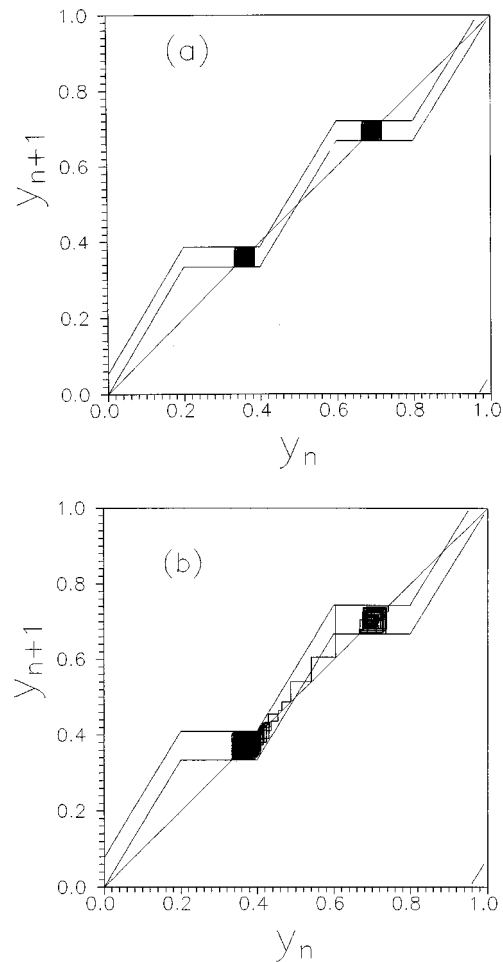


FIG. 3. (a) Orbits for the randomly shifted piecewise linear map (2.6) with $B=0.8 < B_c$. The two orbits are bounded respectively in the two separated bands. (b) Orbit for the map (2.6) with $B=1.15 > B_c$ starting from the lower band. The orbit bounces back and forth and transmits finally to the higher band through the tunnel appearing between the graph of the map and the 45° line. Here $B=15b$ and $B_c=15b_c=1.0$.

negative) x_1 can now switch between two sides of the point $x_1=0$ freely. Typical orbits are shown in Fig. 5.

If a Gaussian noise is used to take the place of the source term $\sin(x_2/2)$ in Eq. (2.9), the subsystem x_1 is just the usually used model to study the stochastic switch in the bistable system [15,16]. In this case, the maximum value of the noise is infinite. So the switch can happen even for a very weak noise strength. One would like to think that the mechanism of the stochastic switch is also due to the crisis reported here.

III. CRISIS-INDUCED INTERMITTENCY AND THE SCALING LAW OF THE CHARACTERISTIC TIME

For a boundary crisis, the system exhibits a long period of chaotic transience before its escape. For an interior crisis and a merging crisis, an episodic switching between two (or more) chaotic behaviors of different characters appears when control parameters pass through their critical values. Grebogi *et al.* named these behaviors crisis-induced intermittency. For a properly defined characteristic time, all these cases have good scaling properties. In studying the crisis-induced

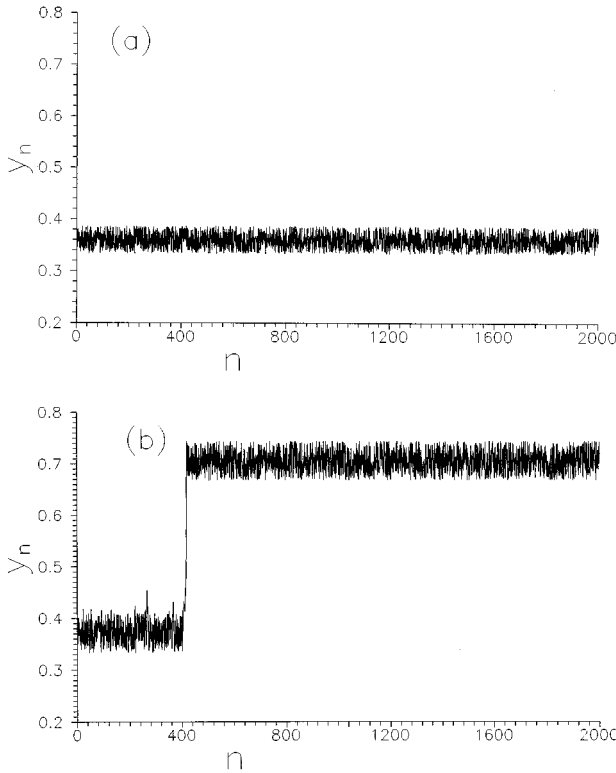


FIG. 4. y_n versus n of model (2.6) for the different values of B : (a) $B=0.08 < B_c$ and (b) $B=1.15 > B_c$.

intermittency, one of the most important problems is to find the critical exponent γ in the scaling law. Below we will use the first two models to illustrate the numerical results about the crisis-induced intermittency and the scaling law for the characteristic times.

It has been pointed out in Sec. II that an uncertain region will appear between the attracting basins of the two coexisting states under the influence of the stochastic term. For the noise strength b beyond a certain critical value b_c , a narrow tunnel appears occasionally between the graph of the map and the 45° line. Let b be slightly greater than b_c and consider an initial condition placed in the phase-space region occupied by the basin of a certain attractor that existed for $b < b_c$ (the lower band in the two models studied here). The orbit starting from this initial condition typically moves toward the region of the $b < b_c$ attractor, moves in a manner reminiscent of an orbit on the $b < b_c$ attractor, and eventually escapes from this region through the narrow tunnel. For $b > b_c$, one of the coexisting attractors is replaced by a chaotic transient. Since there is an uncertain region between the two original attractors, orbits escaping from the phase-space region occupied by the basin of the attractor that existed for $b < b_c$ first enter the uncertain region and remain there for a long time. As a result, two different characteristic times need to be defined. One characteristic is the time an orbit wanders in the phase-space region occupied by the attracting basin of the attractor that existed for $b < b_c$. The second is the time the orbit spends in the uncertain region before it enters other distant attractors. The two times are denoted as τ_1 and τ_2 , respectively, throughout this paper.

An ensemble of orbits starting from the phase points scattered homogeneously in the original attractor, they escape

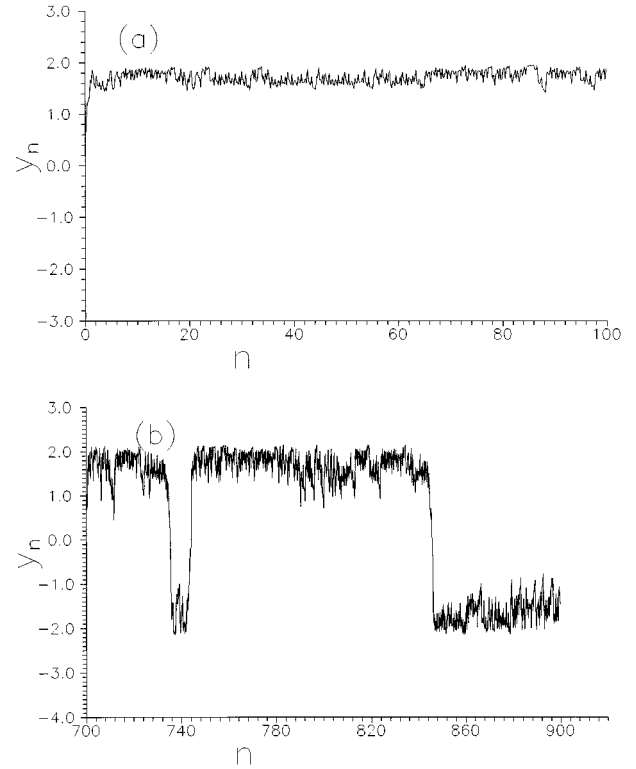


FIG. 5. x_1 versus t of the chaotically driven ODE for values of b : (a) $b=1.5$ and (b) $b=3.8$.

from this attractor one by one through the randomly appearing tunnel. If one records the lifetime of each point staying in the original attractor, the probability distribution of the long lifetime is

$$P(\tau) \sim \exp(-\tau/\langle\tau\rangle). \quad (3.1)$$

So one can get the mean lifetime from the lifetime distribution. Another approach to get the mean lifetime is to calculate it directly. We will use the two approaches to study the dependence of the scaling law of τ_1 and τ_2 on the variation of the control parameter.

For the first model, we start from the randomly selected initial points that are in the interval $[0.515, 0.588]$. Then the map (2.1) is iterated until the value of y_n is greater than a certain value s . The duration of this process is the lifetime we studied. If the value of s is set to 0.588, the abscissa of the tangent point with $b = b_c = 0.03$, the resulting time is the characteristic time τ_1 . If $s = 0.688$, the abscissa of the higher boundary point of the uncertain region, one gets τ_2 . The dependence of the mean lifetimes $\langle\tau_1\rangle$ and $\langle\tau_2\rangle$ on the variation of control parameter are shown in Figs. 6(a) and 6(b). The solid lines to guide eye are of slope 1.20 and 1.48, respectively. This means that $\ln\langle\tau_1\rangle = 1.20\ln(1/\epsilon)$ and $\ln\langle\tau_2\rangle = 1.48\ln(1/\epsilon)$, or $\langle\tau_1\rangle \sim \exp(\epsilon^{-1.20})$ and $\langle\tau_2\rangle \sim \exp(\epsilon^{-1.48})$, where $\epsilon = b - b_c$. Figures 7(a) and 7(b) show the probability distributions of the two characteristic times τ_1 and τ_2 . The figures are constructed by an ensemble of 100 000 examples of the lifetime that is less than 10 000 steps of iteration. To show the exponential decay of $P(\tau)$ for a long lifetime, $P(\tau)$ is plotted in a log-normal frame. It can be easily seen that for large τ , $\ln P(\tau)$ is a perfectly linear

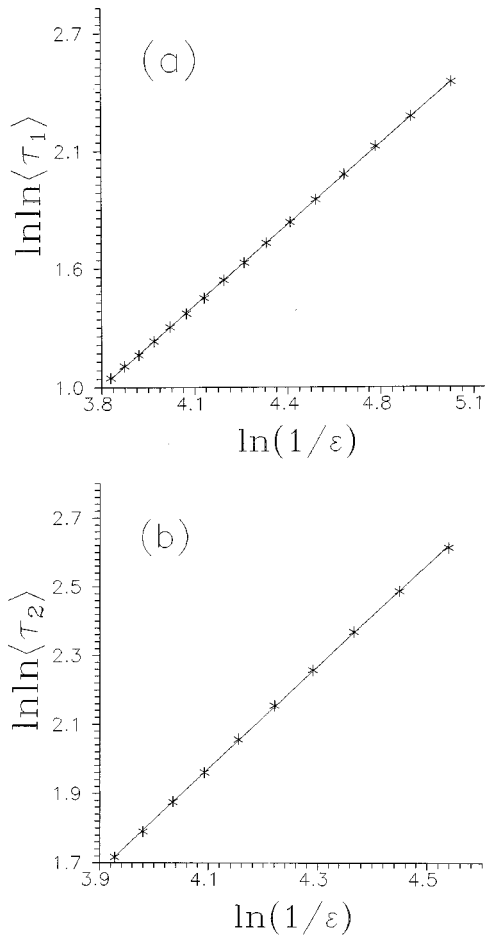


FIG. 6. (a) $\ln \ln \langle \tau_1 \rangle$ versus $\ln(1/\epsilon)$ for model (2.1). The solid line guiding the eyes is of slope 1.20. (b) $\ln \ln \langle \tau_2 \rangle$ versus $\ln(1/\epsilon)$ for model (2.1). The solid line guiding the eyes is of slope 1.48. Each point in the figures is the average of an ensemble of 100 000 examples. The unit of τ is the step of iteration.

function of τ . To fit it to a function $y = k_1 x + k_2$, where $y = \ln P(\tau)$, $x = n$, the dependence of k_1 on $\epsilon = b - b_c$ can be obtained. The solid lines in Figs. 8(a) and 8(b) show that $\ln \ln 1/k_1 = \gamma \ln 1/\epsilon$, with $\gamma = 1.24$ and 1.47 for τ_1 and τ_2 , respectively. From Eq. (3.1) we know that $k_1 \sim 1/\langle \tau \rangle$. So we have $\langle \tau \rangle \sim \exp(\epsilon^{-\gamma})$, with $\gamma = 1.24$ and 1.47 for τ_1 and τ_2 , respectively. The two exponents agree very well with the ones calculated through another approach.

For the second model, initial points are randomly selected in the interval $[0.333, 0.4]$. Also 100 000 examples of the lifetime that is less than 10 000 steps of iteration are used. Similar results for the mean lifetime and the lifetime distribution to the first model are obtained. The mean lifetime $\langle \tau_2 \rangle$ varies as $\langle \tau_2 \rangle \sim \exp(\epsilon^{-\gamma})$, with $\gamma = 0.8$, while another characteristic time increases at a power law with the decrease of ϵ : $\langle \tau_1 \rangle \sim \epsilon^{-0.95}$. From above numerical calculation, one can see that τ_2 increases exponentially with the decrease of ϵ ,

$$\langle \tau_2 \rangle \sim \exp(\epsilon^{-\gamma}), \quad (3.2)$$

and the critical exponent γ depends on the form of the map, while the dependence of another characteristic time τ_1 on ϵ is more variable for different models.

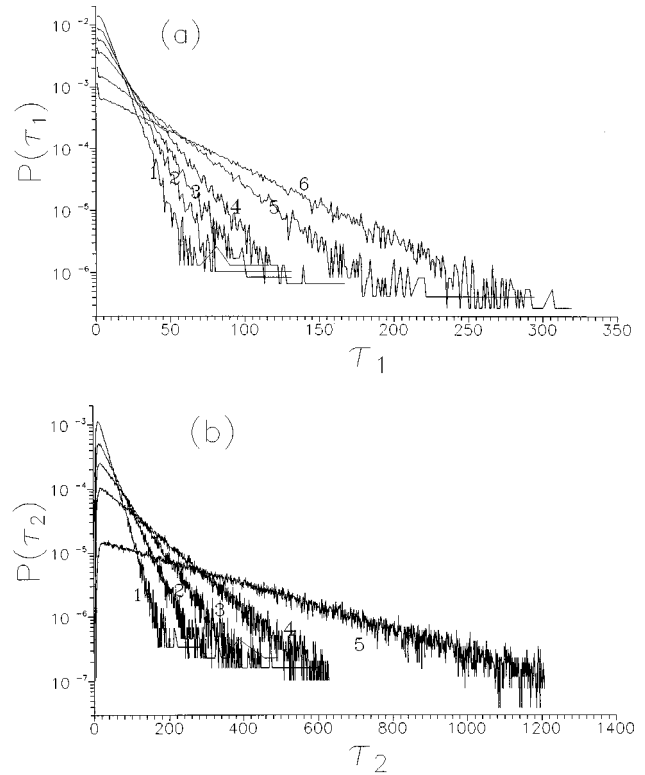


FIG. 7. (a) Probability distribution $P(\tau_1)$ versus τ_1 in model (2.1) with $\epsilon = 0.057, 0.055, 0.053, 0.05, 0.048,$ and 0.045 . The curves are denoted by 1, 2, 3, 4, 5 and 6 respectively. (b) Probability distribution $P(\tau_2)$ versus τ_2 in model (2.1) with $\epsilon = 0.057, 0.055, 0.053, 0.05,$ and 0.048 . The curves are denoted by 1, 2, 3, 4, and 5, respectively. The exponentially decay of $P(\tau)$ at large τ can easily be seen in the figures. The decay rate increases with decreasing ϵ . The unit of τ is the step of the iteration.

IV. SUMMARY AND DISCUSSION

The mechanism of the present crisis is different from the previously reported cases. For the previously reported cases, the crises are triggered by the collision of the chaotic attractor with an unstable attractor or its stable manifold, while the trigger of the present crisis reported here is the ‘‘tunnel effect’’ induced by a backward tangent bifurcation. For the previously reported crises, the orbit colliding with the unstable attractor or its stable manifold is repelled out of the original attractor by the unstable manifold of the unstable orbit. Under the repellent force of the unstable manifold, the orbit inevitably goes to other attractors. The movement of the phase point is in one direction, while for the present crisis, the orbits escape from the original attractor via the randomly appearing tunnel. For the random variation of the parameter, the orbits escaping from the original attractor move back and forth randomly. The movement of the phase points is in two directions. This is the essential difference of the two types of crises. Due to this difference we call them ‘‘collision crises’’ (the previously reported cases) and ‘‘tunnel crises’’ (the case reported here), respectively. The ‘‘unstable-unstable bifurcation crisis’’ reported by Grebogi *et al.* [17] may belong to the later group.

From above numerical calculations, one knows that the characteristic time τ_2 increases exponentially with the decrease of ϵ . The appearance of the super long characteristic

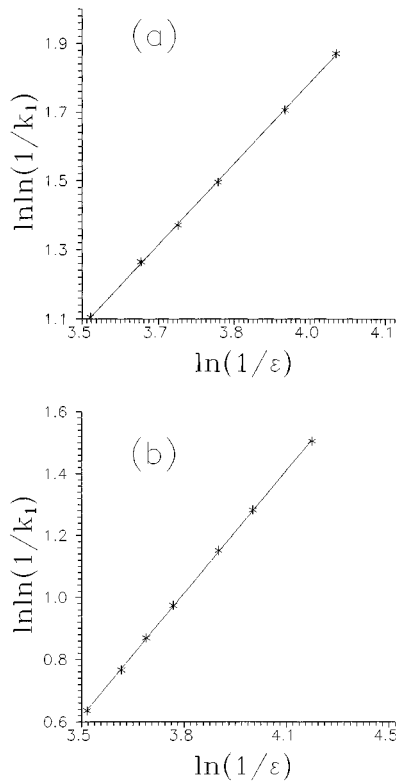


FIG. 8. $\ln \ln(1/k_1)$ versus $\ln(1/\epsilon)$ for k_1 from (a) the fit of the distribution in Fig. 7(a) to $\ln P(\tau_1) = k_1 \tau_1 + k_2$ (the solid line is of slope 1.24) and (b) the fit of the distribution in Fig. 7(b) to $\ln P(\tau_2) = k_1 \tau_2 + k_2$ (the solid line is of slope 1.47).

time is due to the distinctive mechanism of the present crisis. Since the orbit moves back and forth randomly in the tunnel, the time taken to reach the boundary of the uncertain region is very long. Also, the lasting appearance of the tunnel when the phase points escape via it is of very small probability. This is the second factor that makes the characteristic time super long. Since the escape of the phase points from the

original attractor is though a narrow tunnel induced by a tangent bifurcation, just like Pomeau's type-I intermittency, the intermittency induced by the tunnel crisis has some characteristics similar to that of Pomeau's type-I intermittency [18]. The dependence of the critical exponent on metric universality may be one of these characteristics. More detailed research must be done on this dependence.

The power-law dependence of $\langle \tau_1 \rangle$ on ϵ in model (2.9) is only a special case. For this case, the orbits need only one step to go out of the original attractor. The condition for the escape of phase points is just $b > b_c$. Since the value of b distributes homogeneously in $[0, b_c + \epsilon]$, the probability for escape of an orbit from the original attractor is $p \sim \epsilon / (b_c + \epsilon)$. For a system that is very near the critical state, i.e., $\epsilon \ll b_c$, the probability $p \sim \epsilon / b_c$. Then, the lifetime, which is just the inverse of the probability, acts as $\tau_1 \sim 1/p \sim 1/\epsilon$.

It should be noted that all the models in this paper are the one-dimensional case. One is the chaotically driven ODE, the other two are the randomly shifted maps. The common features of them are that they all have a driving noise of a finite maximum value and a pair of stable states separated by an unstable state. Under the driving of the random (or chaotic) noise, one of the stable states and the unstable state approach each other. They annihilate finally due to a backward tangential bifurcation. The backward bifurcation is induced by the random variation of the control parameter. Due to the annihilation, the boundary of the original attractor disappears occasionally. Then the orbits are able to escape through this randomly appearing "hole." This is just the tunnel crisis in one-dimensional systems. What will happen in a high-dimensional system is still an open problem.

ACKNOWLEDGMENTS

This project is supported by the National Nature Science Foundation, the National Basic Research Project "Nonlinear Science," and the Education Committee of the State Council through the Foundation of Doctoral Training.

-
- [1] E. Ott, *Chaos in Dynamical Systems* (Cambridge University Press, New York, 1993), p. 277.
 - [2] C. Grebogi, E. Ott, and J.A. Yorke, *Phys. Rev. Lett.* **48**, 1507 (1982), and references therein.
 - [3] C. Grebogi, E. Ott, F. Romerías, and J.A. Yorke, *Phys. Rev. A* **36**, 5365 (1987).
 - [4] J.C. Sommerer, E. Ott, and C. Grebogi, *Phys. Rev. A* **43**, 1754 (1991).
 - [5] J.C. Sommerer, W.L. Ditto, C. Grebogi, E. Ott, and M.L. Spano, *Phys. Rev. Lett.* **66**, 1947 (1991).
 - [6] Y.C. Lai, C. Grebogi, R. Blümel, and I. Kan, *Phys. Rev. Lett.* **71**, 2212 (1993).
 - [7] M. Toda, *Phys. Rev. Lett.* **74**, 2670 (1995).
 - [8] H.B. Stewart, Y. Ueda, C. Grebogi, and J.A. Yorke, *Phys. Rev. Lett.* **75**, 2478 (1995).
 - [9] H.L. Yang, Z.Q. Huang, and E.J. Ding, *Phys. Rev. Lett.* **77**, 4899 (1996).
 - [10] L.M. Pecora and T.L. Carroll, *Phys. Rev. Lett.* **64**, 821 (1990).
 - [11] J.F. Heagy and S.M. Hammel, *Physica D* **70**, 140 (1994).
 - [12] O. Tai, C. Skorupka, and L.M. Pecora, *Phys. Lett. A* **187**, 175 (1994).
 - [13] L.M. Pecora and T.L. Carroll, *Phys. Rev. Lett.* **67**, 945 (1991); *Phys. Rev. E* **48**, 2426 (1993), and references therein.
 - [14] W.M. Yang, M. Ding, and G. Hu, *Phys. Rev. Lett.* **74**, 3955 (1995).
 - [15] H. Risken, *The Fokker-Plank Equations* (Springer, New York, 1983).
 - [16] H.A. Kramers, *Physica* **7**, 284 (1940).
 - [17] C. Grebogi, E. Ott, and J.A. Yorke, *Phys. Rev. Lett.* **50**, 935 (1983).
 - [18] Y. Pomeau and P. Manneville, *Commun. Math. Phys.* **74**, 189 (1980).